

NANOPARTICLE-ENHANCED PROTON COMPUTED TOMOGRAPHY: A MONTE CARLO SIMULATION STUDY

Reinhard Schulte¹, Vladimir Bashkirov¹, Tianfang Li², Zhengrong Liang², Hartmut F-W. Sadrozinski³, and David C. Williams³

¹ Department of Radiation Medicine, Loma Linda University Medical Center, Loma Linda, CA

² Department of Radiology, State University of New York Stony Brook, Stony Brook, NY

³ Santa Cruz Institute for Particle Physics, University of California at Santa Cruz, Santa Cruz, CA

ABSTRACT

Proton computed tomography (pCT) has the potential to improve the accuracy of proton treatment planning, which is currently based on x-ray computed tomography (xCT). However, at this time no method exists for pCT to selectively increase the contrast of tumor tissues with respect to normal tissues. One possibility to achieve this goal is to bind gold-nanoparticles, i.e., microscopic structures in the size range of 1 nm to several hundred nanometers, to the surface of tumor cells with cell-seeking antibodies conjugated to the surface of the nanoparticles. In order to test the suitability of this approach, we used the Monte Carlo transport code GEANT4, to provide simulated histories of 200 MeV protons going through a cylindrical water phantom with embedded inhomogeneities enhanced with traces of gold. The energy loss of several million protons traversing the cylinder from 180 different angles formed the basis for reconstructing the a single proton CT image representing the relative volume electron density map of the phantom using an approximate filtered back projection algorithm. Our results demonstrate that with hundred nanoparticles of 100 nm diameter per tumor cell, it may be possible to enhance the visibility of tumors in pCT.

1. INTRODUCTION

Over the last two years, we have begun to systematically study the application of proton computed tomography in proton radiation therapy. All existing proton treatment centers are currently using x-ray CT (xCT) to define tumor boundaries and to calculate proton treatment plans. The use of xCT for this purpose is based on the premise that xCT linear attenuation values can be converted to proton stopping power values. Calculation of proton treatment plans based on pCT would, however, be more accurate allowing the radiation oncologist to reduce distal

margins added to the planned target volume to account for proton range uncertainties.

One disadvantage of pCT is the lack of a suitable contrast medium that selectively enhances in tumor tissue. In xCT, high-attenuation contrast media containing iodine are readily available, which typically enhance in tumor tissues due to the modified architecture of tumor vessels. In pCT, however, such contrast media do not exist.

The aim of the present study was to explore the possibility to enhance the density of tumors by binding gold-nanoparticles to the surface of tumor cells using cell-seeking antibodies conjugated to the surface of the nanoparticles. Density-enhanced tumor tissue could then be identified with pCT.

2. METHODS AND MATERIALS

Nanoparticles (Fig. 1) are microscopic structures in the size range of 1 nm to several hundred nanometers, which can be produced with modern nanotechnology techniques.

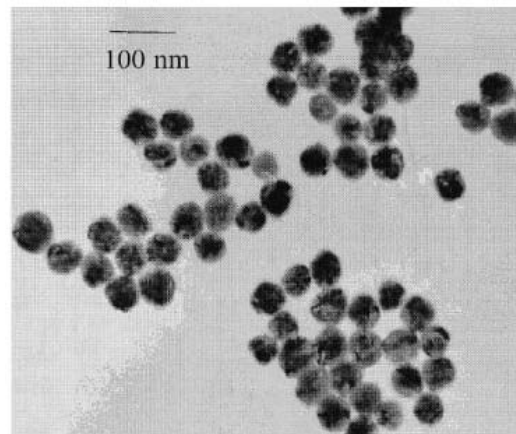


Fig. 1. Transmission electron microscopy image of 60 nm gold nanoparticles (reproduced from [1])

2.1. Back-of-the-Envelope Calculation

One gram of a typical solid tumor contains about 10^9 tumor cells [2]. Halas [3] estimated that *several hundred* antibody-coated nanoparticles can be attached to the

surface of a tumor cell match the antibodies seek their matching antigens on tumor cells. Since not every cell may be loaded, we will conservatively assume that each tumor cell surface carries 100 solid gold nanoparticles.

For a contrast enhancement of 1% one needs to add 10 mg gold or 3×10^{18} gold atoms (atomic weight 196) to 1 cm³ of tumor tissue, assuming unit density. With 10^9 cells and 100 nanoparticles per cell this means that each nanoparticle should carry 3×10^8 gold atoms. A gold nanoparticle of 10 nm diameter carries about 3×10^5 gold atoms [1]. In order to contain 3×10^8 gold atoms, the nanoparticle, therefore, needs to have a diameter of about 100 nm, which is feasible.

2.2. GEANT4 Simulation

Simulated pCT scan data were generated by the GEANT4 Monte Carlo (MC) simulation code [4]. The geometry module of GEANT4 was used to generate a cylindrical water phantom of 20 cm diameter with three 1-cm high gold-enhanced cylinders (Fig. 2, table I).

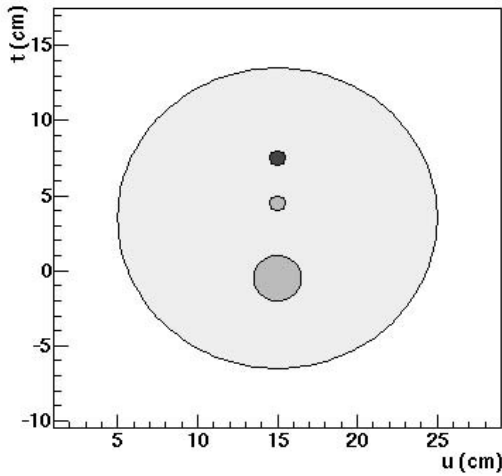


Fig. 2. Reference system for the GEANT4 simulation. The phantom is centered at $u = 15$ cm, $v = 3.5$. The protons arrive along the u direction at plane $u=0$ cm. The proton detector is at $u=30$ cm.

Table I. Phantom Inhomogeneities

$u(\text{cm})$	$t(\text{cm})$	Diameter (cm)	Total amount of gold (mg)	Density enhancement
15	4.5	1.0	10	1.3%
15	-0.5	3.0	90	1.3%
15	7.5	1.0	100	12.7%

The MC program simulated the transport of a total of 6.3 million 200 MeV parallel, mono-energetic protons arriving at the plane $u = 0$ cm with random vertical positions t , ranging from $t = 0$ cm to $t = 7$ cm, and being

detected at the plane $u = 30$ cm. The proton histories were equally distributed over 180 projections ($0 - 360^\circ$, 35,000 protons per projection). The GEANT4 simulation provided the location and direction of exiting protons as well as their residual energy.

2.3. Proton Path Estimation

While traversing the phantom protons undergo multiple small deflections by the Coulomb field of the nuclei, and the path of each proton deviates from a straight line. For the estimation of the proton path, we used the line L determined by the entry and exit positions, provided that we know both the position and direction of the exiting proton, and that the object boundary is roughly known, see Fig. 3.

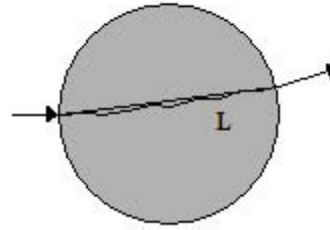


Fig. 3. Illustration of the proton path estimation. Taking into account both entry and exit position one approximates the zigzag proton trajectory by straight line L connecting entry and exit point on the phantom.

2.3. Image Reconstruction

The mean rate of the proton energy loss per unit track length, i.e., the stopping power, is given by the Bethe-Bloch equation:

$$-\frac{dE}{dx}(\mathbf{r}) = \eta_e(\mathbf{r}) F(I(\mathbf{r}), E(\mathbf{r})) \quad (1)$$

where $\eta_e(\mathbf{r})$ is the electron density relative to water, \mathbf{r} represents the spatial location, $I(\mathbf{r})$ is the mean ionization potential of the medium, $E(\mathbf{r})$ is the proton energy, which changes with \mathbf{r} as the proton travels through the body, and F is a known function of I and E defined by the Bethe-Bloch equation [5]. With reasonable assumptions and approximations, the non-linear differential equation (1) can be integrated as

$$\int_{E_{in}}^{E_{out}} \frac{dE}{F(I_{water}, E)} = \int_L \eta_e(\mathbf{r}) dl \quad (2)$$

which would be in the format of the Radon transform if proton paths were straight lines confined to a 2D plane: the right side is the line integral of the relative electron density along the proton path L , and the left side is a unique function of the proton energy difference. In equation (2), $I(\mathbf{r})$ was replaced by the mean ionization potential of water $I_{water} = 61.77$ eV. This is justified because in human tissues the variation of I is not very

large and the dependence of the function F on I is relatively weak.

Using equation (2) to convert proton energy loss into integrated relative electron density, the phantom density reconstruction was performed by the conventional filtered backprojection (FBP) method. To apply the conventional FBP reconstruction algorithm for the randomly arriving protons, it was necessary to interpolate the projection rays L in order to fill a uniform sinogram space. The bilinear interpolation method was used according to the pixel-distances in the sinogram.

3. RESULTS

Fig. 4 shows the reconstructed phantom image (see Fig. 2 for comparison) based on 6.4 million proton histories. While the object with 12% density enhancement is very well distinguished from the background water signal, the other two objects with 1.2% gold-density enhancement are only faintly visible. One should note the absence of any artifacts in the reconstructed image.

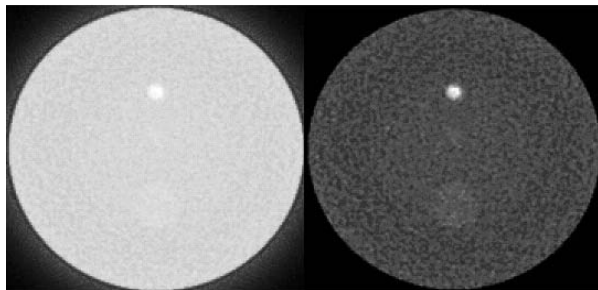


Fig.4. Reconstruction result for gold-enhanced pCT simulations. Left: full-window display; Right: 30% window display.

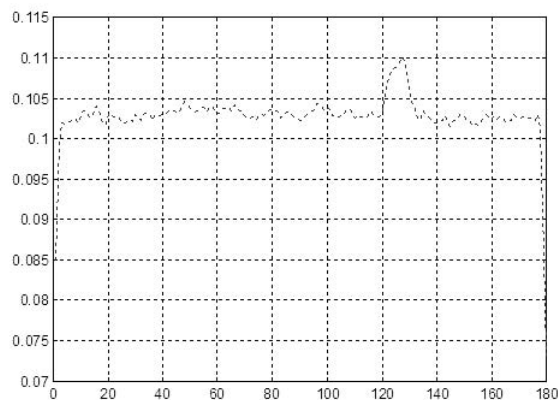


Fig.5. Electron density profile of Fig. 4 along the central vertical line. The upper (1 cm diameter, 12% density enhanced) gold-water cylinder is best revealed.

Fig. 4 and 5 demonstrate that for the conditions under which these pCT images were simulated, the 1.2% density enhanced objects are near the limit of visibility due to the

presence of image noise. It is important in this respect to consider the dose that was delivered to the phantom to generate these images. The total proton energy lost in the phantom was 4.5×10^8 MeV. Assuming that this energy was distributed over a slice of 1 mm thickness with a corresponding mass of 0.31 kg, the average dose to the phantom is 2.27×10^{-4} Gy per projection or 4.54×10^{-2} Gy (4.5 cGy) for the full scan.

4. DISCUSSION AND CONCLUSION

Our simulation study is a first attempt to test the idea of enhancing the density of tumors with gold-nanoparticles with the intent to improve their visibility in pCT. This would allow to fully exploit the greater accuracy of pCT for proton treatment planning. For the low contrast enhancement tested in our simulation (1.2%) and a dose of 4.5 cGy, which is in the lower range of typical single-slice doses of modern xCT scanners, the enhanced cylindrical objects of 1 cm and 3 cm were at the limit of visibility. Improved visibility can only be achieved by increasing the dose, which may be acceptable for cancer patients, or by increasing the nanoparticle load per tumor cell, which may be technically difficult.

Our study indicates that experimental studies with nanoparticle labeled tumor tissues and experimental pCT systems should be performed to test the feasibility of this approach.

5. REFERENCES

- [1] S. Link and M. A. El-Sayed, "Shape and size dependence of radiative, non-radiative and photothermal properties of gold nanocrystals," *Annu. Rev. Phys. Chem.*, Vol. 19, No. 3, pp 409-453, 2000.
- [2] Hall E. *Radiobiology for the Radiologist*. Lippincott Williams & Wilkins, Philadelphia, 2000.
- [3] L.R. Hirsch, R. J. Stafford, J.A. Bankson, S.R. Serksen, B. Rivera, R.E. Price, J.D. Hazle, N.J. Halas, and J.L. West, "Nanoshell-mediated near-infrared thermal therapy of tumors under magnetic resonance guidance," *Proc Natl Acad Sci U S A* Vol. 100, No.23, pp 13549-13554, 2003.
- [4] S. Agostinelli, et al., "GEANT4 - A Simulation Toolkit *NIM A*, Vol. 506, no. 3, pp. 250-303, 2003.
- [5] H. Bichsel, "Passage of charged particles through matter," *American Institute of Physics handbook*, vol. 42, B. H. Billings, D. E. Gray, et al., Eds. McGraw-Hill, New York, 1972.